J. Coat. Technol. Res., **18** (5) 1245–1259, 2021
https://doi.org/10.1007/s11998-021-00485-x

The preparation of superhydrophobic photocatalytic fluorosilicone/SiO_2–TiO_2 coating and its self-cleaning performance

Lijun Zong, Yaping Wu, Xingeng Li, Bo Jiang

Received: 26 May 2020 / Revised: 8 February 2021 / Accepted: 15 February 2021

Abstract In this study, superhydrophobic photocatalytic fluorosilicone/SiO_2–TiO_2 (FSi/SiO_2–TiO_2) coatings were prepared. Evolutions of wettability and photocatalytic activities were explored by exposing a series of samples to UV irradiation and the outdoor environment. Their practical self-cleaning performances were also compared. The UV-irradiation test was carried out in an ultraviolet aging test chamber. Wetting properties, including water contact angles and sliding angles, were measured using a contact angle meter. A UV spectrophotometer was employed to detect and evaluate the coatings' photocatalytic properties. Moreover, morphologies and surface roughness values were tested through field emission scanning electron microscope and optical profilometer, respectively. It is shown from experimental results that the coating series with more TiO_2 addition amounts transform from superhydrophobic to superhydrophilic in a shorter time. The coating with a more durable superhydrophobicity can maintain its initial wettability, while its photocatalytic property is superior to that of a hydrophobic coating. Mechanisms were put forward through analyzing the coating microstructures. It is considered that the superhydrophobic coating with a Cassie–Baxter surface structure shows a better photocatalysis. Besides, it has been confirmed that the practical self-cleaning performance of the prepared superhydrophobic photocatalytic FSi/5TiO_2–32SiO_2 coating is better in comparison with superhydrophobic FSi/SiO_2 and photoinduced superhydrophilic FSi/5TiO_2–28SiO_2 coatings.

L. Zong (✉), Y. Wu, X. Li, B. Jiang
State Grid Corporation Joint Laboratory of Advanced Electrical Engineering Material (SDEPC), State Grid Shandong Electric Power Research Institute, Jinan 250000, China
e-mail: dkyzonglijun@163.com

Keywords Photocatalytic activity, Superhydrophobic, Self-cleaning, TiO_2, Fluorosilicone resin

Introduction

Self-cleaning properties are usually used to evaluate the abilities of a surface to remain clean. Pollutants could fall off or be degraded with external forces such as wind, light and rainfall. It is known that self-cleaning performances can be achieved through either superhydrophobicity or superhydrophilicity.[1–4] It is well known that a superhydrophobic surface has a water contact angle more than 150° and a sliding angle less than 10°. During the last decades, studies and research on superhydrophobic surfaces have emerged endlessly.[5–7] Inspired by lotus leaves, all kinds of artificial superhydrophobic surfaces are fabricated by low surface energy components with a hierarchical roughness. Practical applications of superhydrophobic surfaces have been deeply investigated, especially for efficient self-cleaning applications.[8–11] Real contact area between a water drop and a superhydrophobic surface is significantly reduced due to the air entrapped in its hierarchical micro/nanostructure.[12] Water on superhydrophobic surfaces seems to be lifted by small air bags, and thus, droplets can easily roll off the surface. Dust particles or pollutants can be taken away by the rolling down of water droplets.[13,14] Dry powders were generally employed as contaminants to test the self-cleaning property, such as graphite powder,[15,16] charcoal powder,[17] heavy iron powder,[18] and even black pepper powder.[19] Artificial dirty solutions were also studied by some researchers.[20] However, the pollutants in nature appear with various characteristics. Most superhydrophobic surfaces are usually oleophilic and apt to be contaminated by organic pollutants. Although a superamphiphobic surface could help repel organic pollution, its application is limited owing to complicated and expensive processes.[21,22] Nevertheless, the organic

pollutants can be chemically decomposed through a ''photocatalysis'' process, which provides an alternative method of self-cleaning.[23]

Photocatalytic activity is one promising technology to achieve self-cleaning effect through which organic contamination can be decomposed.[25,26] It is well known that TiO_2 has been intensively investigated due to its high stability, nontoxicity, low cost and efficient photocatalytic activity.[27–29] TiO_2 with a band-gap energy of 3.2 eV can absorb UV light. Upon UV light exposure, a positive electron hole (h^+) is generated in the valence band when a photoexcited electron (e^-) hops from valence band to conduction band. Redox reactions are carried out on the electrons and holes with oxygen and water, and thus, radicals, such as superoxide ion and hydroxyl radical, are formed. The organic pollutants can be decomposed into CO_2 and H_2O by these reactive oxygen species (ROS), which is favorable to surface self-cleaning effect.

It is novel to introduce TiO_2 properties into superhydrophobic surfaces to enhance self-cleaning effects. Research on TiO_2 films with superhydrophobicity is mainly divided into two typical fields. One study is concentrated on the reversible wettability switching between superhydrophobicity and superhydrophilicity. Ever since the photoinduced wettability change on TiO_2 surfaces was first discovered,[4] relevant studies have paid more attention to the wettability switching of TiO_2 surfaces.[34–36] In addition, some research focuses on fabrication of the superhydrophobic materials with photocatalytic activity.[37–39] Although it is still a challenging task to incorporate TiO_2 particles into a superhydrophobic surface, more and more achievements on superhydrophobic and photocatalytic surfaces have been attained. Kamegawa et al. prepared a TiO_2–PTFE/Ti composite coating with durable superhydrophobicity by RF-MS technique, and the superhydrophobic state could be restored even after cycles of oleic acid adhesion under UV irradiation.[40] Park et al. investigated the dual functionality of superhydrophobicity and photocatalysis on the film containing TiO_2 and PDMS-coated SiO_2 nanoparticles. It was found that when the ratio of PDMS-coated SiO_2 and TiO_2 was 7:3, the film exhibited UV-induced photocatalytic activity and stable superhydrophobicity with a water contact angle of 165°.[41] Ratova and coworkers deposited superhydrophobic photocatalytic PTFE–TiO_2 composite by reactive pDC magnetron sputtering. The deposited coating with the highest static contact angle (CA) of 152° (± 2°) showed better photocatalytic activity compared to titania samples.[42] The surfaces reported in most studies usually exhibited a reversible wetting transition. However, Zhao et al. obtained stable Cassie state superhydrophobic surfaces by embedding TiO_2 particles into printed PDMS arrays. The presented novel method ensured a high catalyst rate and stable superhydrophobicity.[43] Obviously, fabrication methods mentioned above are either complicated or expensive. Although the research on self-cleaning surfaces combining superhydrophobicity with photocatalysis are creative, the fabrication methods restricting the practical application need to be further optimized. The ''one-pot'' preparation and spraying method for fabricating superhydrophobic coatings is worth trying. Professor Zhou and his team have fabricated a long-term superhydrophobic coating by blending PMSF with TiO_2 nanoparticles.[44] After UV irradiation, the contact angle of a polluted coating surface recovered from 62.5° to the superhydrophobic state. The preparation process of superhydrophobic coating with photocatalytic properties should be further investigated by a simple blending method. In addition, the self-cleaning performance of a superhydrophobic photocatalytic surface should be evaluated with a more original approach.

In our previous study, superhydrophobic FSi/SiO_2 coating has been successfully fabricated by a one-step blending method, which showed a self-cleaning characteristic due to superhydrophobicity.[45] In order to improve the self-cleaning performances of superhydrophobic surfaces by introducing photocatalysis, photocatalytic TiO_2 particles are introduced into the coating system in this work. Effects of TiO_2 amounts on the coating wettability changes with the UV irradiation, and outdoor exposure times are investigated, respectively. Effects of initial hydrophobicity on the coating wettability changes are also discussed. In addition, the degradation rates of methylene blue are used to evaluate the UV-driven photocatalytic activity. Finally, self-cleaning properties of the prepared superhydrophobic photocatalytic FSi/SiO_2–TiO_2 coating surface are studied using natural contamination depositing method by sample exposure.

Experimental section

Materials

Fluorosilicone resin (FSi, more than 26% fluoride content) with curing agent was obtained by Dongfu Chemical Technology Co., Ltd. TiO_2 nanoparticles were received from Evonik (Degussa P25), and SiO_2 particles with an average size of 4 μm were from Shouguang Hengtai Company (T604). The 1*H*, 1*H*, 2*H*, 2*H*-perfluorooctyltriethoxysilane (97%, FAS13) was provided by Aladdin. Deionized water was self-made in our own laboratory. Anhydrous ethanol (EtOH), acetic acid (HAc), butyl acetate, ethyl acetate and methylene blue were purchased from Sinopharm Chemical Reagent Co., Ltd. All the reagents were analytical grade and used as received without any further purification.

Sample preparation

(1) *The modification of SiO_2 and TiO_2 particles* First, 0.5 mL of HAc as a catalyst was added into

a mixed solvent of 1 mL deionized water and 9 mL EtOH. Then, 1 mL FAS13 was added dropwise into the mixed solvent, and FAS hydrolysate was produced by stirring the mixture for 60 min. Then, homogenous SiO_2 suspension liquid was obtained by shearing 5 g of SiO_2 particles dispersed in 20 g of EtOH. At last, the FAS hydrolysate was added into the SiO_2 suspension liquid and continuous stirring was performed for 6 h. The obtained solution was cleaned with EtOH by centrifugation for three times and dried at 90°C. Consequently, the modified SiO_2 particles were prepared. The modification process of TiO_2 nanoparticles was the same as that of SiO_2.

(2) *The preparation of superhydrophobic coating with photocatalytic activtiy* First, 3 g of SiO_2 and varying amounts of TiO_2 nanoparticles (0.15 g, 0.3 g, 0.5 g, 0.75 g) were dispersed in mixed solvent of ethyl acetate (12 g) and butyl acetate (10 g) by ultrasonic dispersion for 15 min. Ten grams of fluorosilicone resin was then added to this suspension solution with mechanical stirring for 1 h. Thus, coating component A was in preparation. Subsequently, the coating was obtained by mixing and stirring 1.25 g of curing agent with the component A for 5 min. The coating suspension was sprayed onto a glass substrate with 0.3 MPa compressed air flow using a spray gun (Anest Iwata W-71). Distance between the spray gun and the substrate was about 25 cm. Finally, the coating was cured at ambient temperature for over 24 h. The samples in this experiment group were marked as FSi/30SiO_2–$x$$TiO_2$ coatings (x = 1.5, 3, 5, 7.5). In the other experiment group, 0.5 g of TiO_2 and varying amounts of SiO_2 particles (2 g, 2.4 g, 2.8 g, 3.2 g) were dispersed in the first stage, and coating samples were prepared in the same way as the FSi/30SiO_2–$x$$TiO_2$ coatings. Similarly, the coating samples were assigned to be FSi/5TiO_2–$x$$SiO_2$ (x = 20, 24, 28, 32).

Sample characterization

Filler compositions were determined by X-ray diffractometer (XRD, X'Pert Pro X, PANalytical B.V.). Fourier transform infrared spectrophotometer (FTIR, Magna-IR 560, Nicolet) was used to confirm types of chemical bonds. In order to evaluate the coating hydrophobicity and its variation during UV irradiation and outdoor exposure, water contact angles (WCA) were measured on a contact angle instrument (JCY-4, China) by sessile-drop method. Sliding angles (SA) were tested when necessary. The WCA values were measured using 4 μL water, and the SA values were measured with a droplet volume of 10 μL. The obtained value was an average of five measurements at different positions for each sample.

A UV-irradiation test was carried out in an ultraviolet aging test chamber (UV-290, China). The ultraviolet lamp (UVA-340, ATLAS, USA) could be used to simulate the UV light with a wavelength ranging from 280 to 400 nm. Glass plates (10 cm × 8 cm) coated with the prepared coatings were placed into a UV aging test chamber. Distance between ultraviolet lamp and coating surface was set as 10 cm. In outdoor exposure test, the same batch of glass plates was placed horizontally on a specially made shelf. WCA and SA values were detected with prolonged UV irradiation and outdoor exposure time.

The coating photocatalytic properties were evaluated by methylene blue (MB) degradation test under a radiation intensity of 1 W/m^2. Glass plates coated with films (50 mm × 15 mm × 0.1 mm) were immersed into a 20 mL sample vial full of MB solution (5 mg/L). Photocatalytic degradation of MB was investigated by measuring MB concentrations, which can be calculated from MB absorption spectra at λ_{max} 664 nm detected using a UV spectrophotometer (Evolution 201, Thermo Fisher). In addition, phenol, a typical organic pollutant, was chosen to test the photocatalytic activity of our prepared superhydrophobic photocatalytic FSi/5TiO_2–32SiO_2 coating. The whole degradation test on the phenol solution (10 mg/L) was performed with the same process as for MB degradation test. Concentrations of phenol solution were tested at certain times, and the corresponding removal efficiencies were calculated.

Results and discussion

Effects of TiO_2 addition amount on the wettability change

In order to overcome the vulnerability of superhydrophobic FSi/SiO_2 surfaces being easily contaminated by oil, photocatalytic TiO_2 particles were introduced into the superhydrophobic coating system. The SiO_2 addition amount was kept at a constant of 30%, while TiO_2 doping contents were adjusted from 1.5 to 7.5%. Elemental composition and types of chemical bonds of the FSi/30SiO_2–$x$$TiO_2$ coating series were confirmed by XRD and FTIR spectra, respectively. Figure 1 shows XRD patterns and FTIR spectra of FSi/SiO_2 coatings with different TiO_2 doping contents. It can be seen from Fig. 1a that diffraction peaks of anatase TiO_2 and rutile TiO_2 are observed in the XRD patterns of FSi/30SiO_2–$x$$TiO_2$ coatings. The diffraction peaks of TiO_2 crystals are stronger with increasing TiO_2 addition ratio. A noncrystalline diffraction peak appears between 16° and 24°, which is recognized as amorphous silica. The SiO_2 structure does not change during the modification and dispersion process. Typical chemical bonds can be distinguished from the FTIR spectra of the coating samples presented in Fig. 1b. The infrared absorption bands at about 2940 cm^{-1}, 1464 cm^{-1} and 1374 cm^{-1} in the spectra are ascribed to

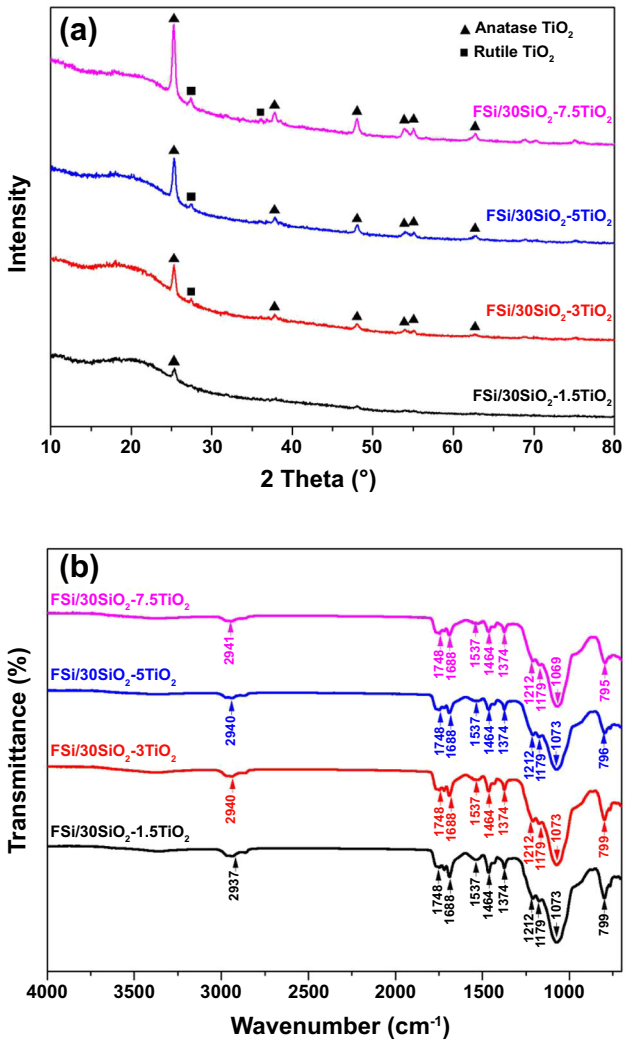

Fig. 1: XRD patterns and FTIR spectra of FSi/SiO_2 coatings with different TiO_2 doping contents: (a) XRD patterns; (b) FTIR spectra.

stretching and deformation vibrations of C–H groups. There are C=O peaks at the wavenumbers 1748 cm^{-1} and 1212 cm^{-1}. The stretching vibrations of C=C bond are observed at 1688 cm^{-1}. An infrared absorption peak at about 1179 cm^{-1} is attributed to the C–F bond. In addition, the FTIR bands at about 1080 cm^{-1} and 799 cm^{-1} are the antisymmetrical and symmetrical stretch vibration absorption spectra of Si–O–Si, respectively. The absorption peaks discussed above show inherent chemical bonds of FSi resin. The absorption peak at 1537 cm^{-1} is characterized as NH–CO bond in the cured resin.

The initial wettability states of FSi/SiO_2 coatings with different TiO_2 doping contents are shown in Fig. 2. It can be seen that all the WCA values of prepared coatings exceed 150° and the SA values are less than 10°, which means that all the prepared FSi/30SiO_2–$x$$TiO_2$ belong to the superhydrophobic coating system. Moreover, the WCA values show a slight decreasing tendency with

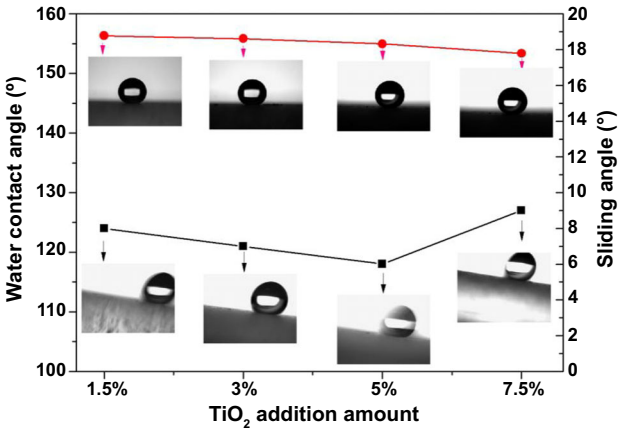

Fig. 2: The initial wettability states of FSi/SiO_2 coatings with different TiO_2 doping contents.

increasing TiO_2 addition. Although the sliding angle of FSi/30SiO_2–7.5TiO_2 coating reaches a relative maximum value, the coating still presents good superhydrophobicity. It can be concluded that the coating superhydrophobicity is not notably impaired by the addition of TiO_2 particles.

The wettability changes of FSi/SiO_2 superhydrophobic coating with different TiO_2 addition amounts were explored under UV irradiation and outdoor exposure. Figure 3 shows the effects of TiO_2 addition amounts on the WCA and SA changes under UV irradiation and outdoor exposure. From Fig. 3a, it can be seen obviously that the WCA values of FSi/30SiO_2–$x$$TiO_2$ coatings are relatively stable in the early stage of UV irradiation. There is no significant change of WCA values during the first 150 h. Downward trends of WCA values are observed after 152 h for the coatings with 3%, 5% and 7.5% of TiO_2 addition amounts, but different decrease rates are shown. A WCA value of 0° is first detected on FSi/30SiO_2–7.5TiO_2 coating after 176 h of UV irradiation. Similarly, the coatings with 3% and 5% TiO_2 addition amounts also present superhydrophilicity with a WCA value of 0° at the 190th hour. Although the added TiO_2 quantity is low, the WCA value of FSi/30SiO_2–1.5TiO_2 coating starts to decrease from the 190th hour. It is worth noting that all the SA values increase sharply within 40 h, as shown in Fig. 3b. The SA value of coating sample with 7.5% TiO_2 increases to 45° within 10 h. The SA of sample with 3% TiO_2 increases linearly and almost reaches 30° in 20 h. The SA values of coatings with dosages of 1.5% and 5% change slowly during 30 h and increase sharply in the following 10 h. It is found that the WCA and SA values of outdoor samples display quite similar changing trends as that under UV irradiation, as seen from Figs. 3c and 3d. Although all the outdoor coatings would eventually turn into superhydrophilic, the time points when WCA values begin to decrease are more advanced. Furthermore, the SA values of FSi/30SiO_2–7.5TiO_2 coating increase more sharply and the corresponding superhydrophilic coating can be obtained in a shorter time.

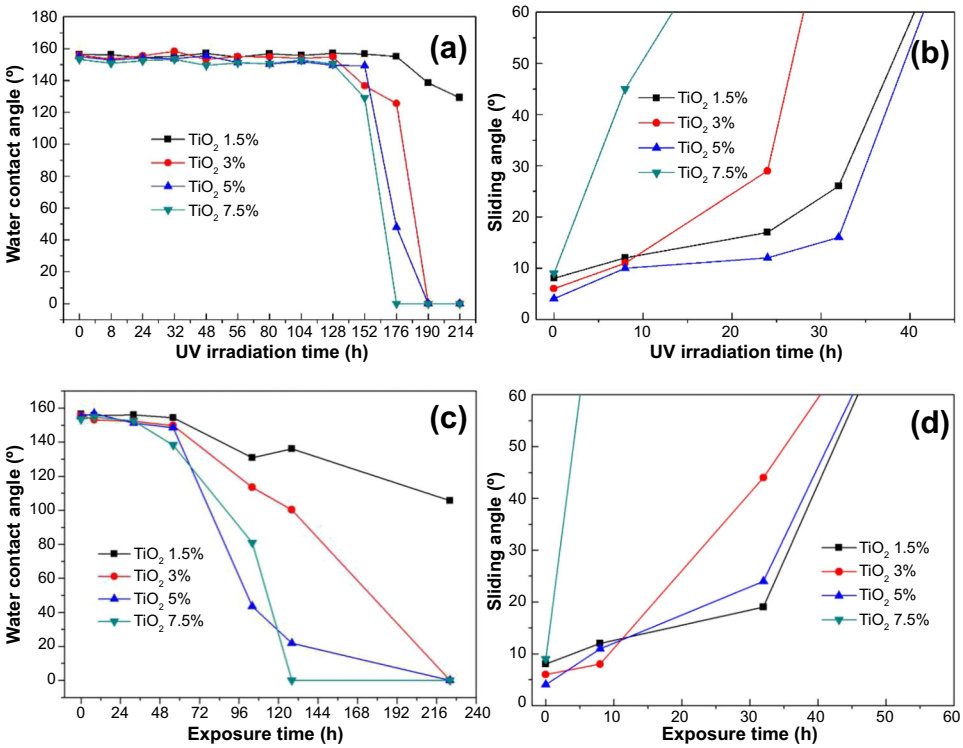

Fig. 3: Effects of TiO_2 addition amount on the wettability changes under UV irradiation and outdoor exposure: (a) WCA changes under UV irradiation; (b) SA changes under UV irradiation; (c) WCA changes under outdoor exposure; (d) SA changes under outdoor exposure.

There is no doubt that TiO_2 plays a key role in the surface characteristics for wettability change. It has been revealed that the photoinduced hydrophilicity of TiO_2 films originates from its peculiar surface microstructure. The formation of Ti-OH groups is promoted during the irradiation process according to semiconductor energy band theory, which could significantly enhance the absorption of water molecules.[46] Therefore, the coating surfaces would transform from superhydrophobic to superhydrophilic. With an increased TiO_2 portion, the superhydrophobic nature of the coating surface could only be maintained for a shorter time. Compared with the UV-irradiation group, the WCA values of coating samples under outdoor exposure decrease more quickly due to higher humidity in the outdoor environment. A significant decrease of WCA values for outdoor exposure coatings has been detected at about the 96th hour, which can be attributed to the higher humidity on a rainy day. The TiO_2 addition could be favorable for not only introducing the photocatalyst effect but also for constructing the superhydrophobic structure. TiO_2 particles with the addition proportion of 5% tend to have an influence on the coating microstructure. It can be found that the primary SA value of FSi/30SiO_2–5TiO_2 coating is less than that with 3% TiO_2, and the SA value of FSi/30SiO_2–5TiO_2 coating would change later under UV and outdoor exposure.

Effects of SiO_2 addition amount on the wettability change

According to the above results, it could be concluded that the coating superhydrophobicity would be lost even if the TiO_2 addition proportion is as low as 1.5%. Therefore, the effect of the initial hydrophobicity on the coating wettability change should be investigated. As is known, a superhydrophobic surface is able to be obtained by low surface energy film and a structure with hierarchical roughness. SiO_2 nanoparticles were successfully used to construct superhydrophobic surfaces in many studies.[47,48] Thus, SiO_2 particles were employed to adjust the initial hydrophobicity of the coatings in this study. SiO_2 doping ratios were adjusted from 20 to 32%, and TiO_2 addition ratio was kept at a constant of 5%. Elemental composition and types of chemical bonds of FSi/5TiO_2–$x$$SiO_2$ coating series were confirmed by XRD and FTIR spectra, respectively. Figure 4 shows the XRD patterns and FTIR spectra of FSi/TiO_2 coatings with different SiO_2 doping contents. It can be seen that the elemental position and chemical bonds of FSi/5TiO_2–$x$$SiO_2$ coatings are similar to those of FSi/30SiO_2–$x$$TiO_2$ samples. The diffraction peak intensities of TiO_2 among FSi/5TiO_2–$x$$SiO_2$ coatings are close to each other due to the same filler amounts.

The initial wettability states of FSi/TiO_2 coating with different SiO_2 doping contents are shown in Fig. 5.

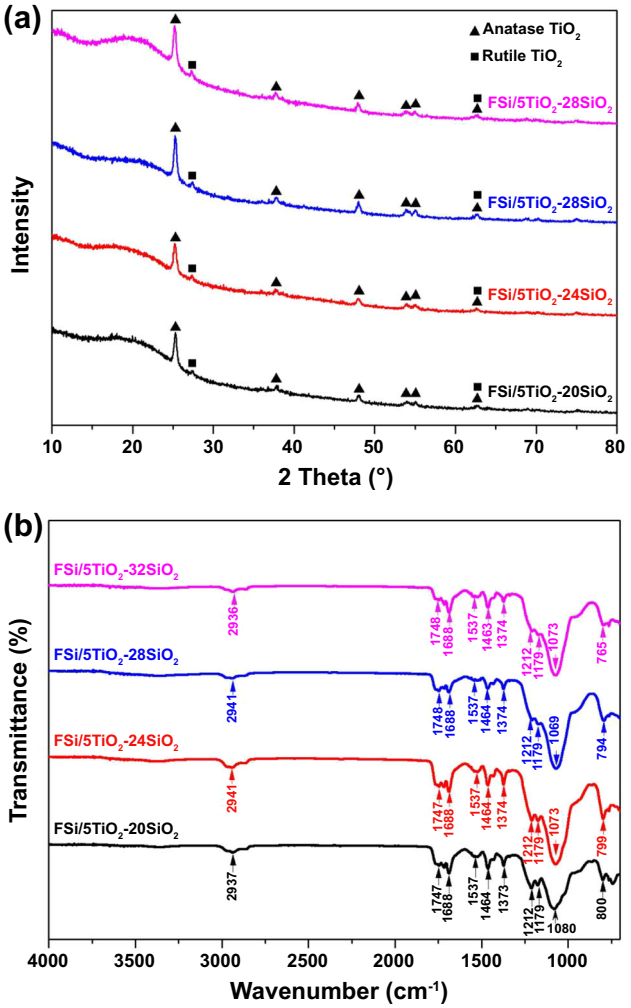

Fig. 4: XRD patterns and FTIR spectra of FSi/TiO_2 coating with different SiO_2 doping contents: (a) XRD patterns; (b) FTIR spectra.

Clearly, the coating hydrophobicity is gradually improved with increasing SiO_2 contents, presented as increasing WCA values and decreasing SA values. Furthermore, more detailed information can be observed in Fig. 5. The coating with 20% SiO_2 shows a WCA value of 122.38° and an SA value larger than 180°, while the WCA value of the $FSi/5TiO_2$–$24SiO_2$ coating exceeds 150° and its SA is measured as 34°. The WCA and SA values of the $FSi/5TiO_2$–$28SiO_2$ coating are detected as 154.92° and 6°, respectively, and the $FSi/5TiO_2$–$32SiO_2$ coating possesses a WCA value of 158.37° and SA value of 3°. Although the superhydrophobicity can be obtained on the coating with both 28% and 32% of SiO_2 addition, a larger WCA value and a smaller SA value are shown for the $FSi/5TiO_2$–$32SiO_2$ coating.

As mentioned above, the wettability changes of FSi/TiO_2 coating with different SiO_2 addition amounts should also be explored under UV irradiation and outdoor exposure. Figure 6 shows the effects of SiO_2

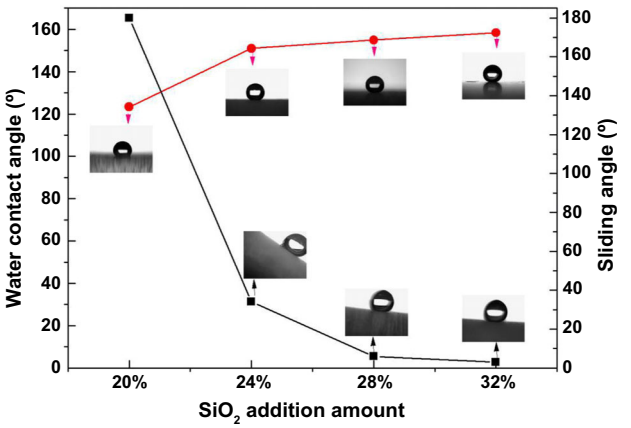

Fig. 5: The initial wettability states of FSi/TiO_2 coating with different SiO_2 doping contents.

addition ratios on WCA and SA evolution under UV irradiation and outdoor exposure. There is quite a difference concerning the time when WCA begins to decrease for coating samples with different SiO_2 addition ratios, as seen from Fig. 6a, which must be determined by their initial hydrophobicity. The maintaining time of initial WCA values is first shortened and then prolonged with increasing SiO_2 addition ratios. The WCA value of $FSi/5TiO_2$–$20SiO_2$ coating sample begins to decrease obviously at about the 176th hour and then falls gradually to 0°. By contrast, the $FSi/5TiO_2$–$24SiO_2$ coating can hold its initial WCA value for only 48 h. It changes to a superhydrophilic coating with a 0° WCA value at the 80th hour. In addition, the WCA value of $FSi/5TiO_2$–$28SiO_2$ coating has no obvious change within 104 h and then begins to decrease to 0°. However, the $FSi/5TiO_2$–$32SiO_2$ coating can unexpectedly maintain a stable WCA value above 150° for 214 h or even longer. The SA values of $FSi/5TiO_2$–$32SiO_2$ are kept below 10° during this period, shown in Fig. 6b. It could also be seen from Fig. 6b that the SA of FSi/TiO_2 coatings with 24% and 28% of SiO_2 addition ratios increase to values larger than 180° during 12 h. Compared with the coating samples under UV irradiation, the wettability changes under outdoor exposure display a similar behavior, as shown in Figs. 6c and 6d. Generally, the $FSi/5TiO_2$–$20SiO_2$ coating holds a stable WCA value for a relatively longer time, and the SA values of $FSi/5TiO_2$–$24SiO_2$ and $FSi/5TiO_2$–$28SiO_2$ coatings increase significantly in daytime, and both transform to superhydrophilic coatings within 100 h. The $FSi/5TiO_2$–$32SiO_2$ coating exhibits an excellent superhydrophobicity stability under outdoor exposure. It keeps nonwetting even on a rainy day at the 94th hour.

Based on the above results, the durability of a superhydrophobic FSi/TiO_2 coating may not be affected by photocatalytic and superhydrophilic characteristics of TiO_2. However, it is necessary to construct an excellent superhydrophobic state, just like the prepared $FSi/5TiO_2$–$32SiO_2$ coating. The coating can

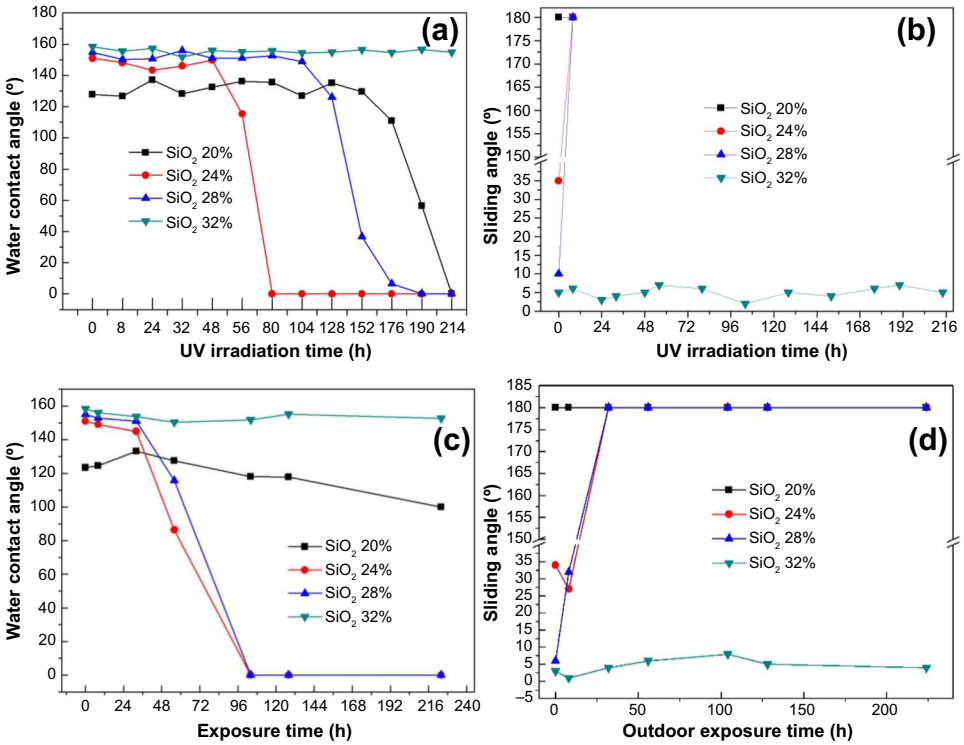

Fig. 6: Effects of SiO_2 addition ratios on the wettability changes under UV irradiation and outdoor exposure: (a) WCA changes under UV irradiation; (b) SA changes under UV irradiation; (c) WCA changes under outdoor exposure; (d) SA changes under outdoor exposure.

transform to superhydrophilic more easily due to poor initial superhydrophobicity, such as the prepared FSi/5TiO_2–24SiO_2 coating. It indeed needs more time to weaken the superhydrophobicity of coatings with good initial superhydrophobicity. However, a superhydrophilic surface is easily obtained once the WCA value begins to decrease, such as the prepared FSi/5TiO_2–28SiO_2 and FSi/30SiO_2–$x$$TiO_2$ coatings.

Photocatalytic degradation performances

In order to confirm and compare photocatalytic performances of the prepared coatings, degradation of methylene blue (MB) diluted in water was investigated under UV light irradiation. The concentrations of MB solution degraded after UV irradiation were detected, and UV–Vis spectra of MB adsorbed were compared. Figure 7 shows the photocatalytic degradation performances of FSi/SiO_2 coatings with different TiO_2 addition ratios, and the corresponding inset figures show the decolorization of MB solution visually. From the spectra and pictures, we can see that all the MB solutions have been degraded by four coating samples with different TiO_2 amounts. However, there is a significant difference among degradation efficiencies of the four coatings. The degradation performance of FSi/30SiO_2–3TiO_2 coating is not obviously better than that of FSi/30SiO_2–1.5TiO_2 coating, while there is an obvious increase of degradation rate as the TiO_2 addition ratio reaches 5%. The degradation efficiency of FSi/30SiO_2–7.5TiO_2 coating is further promoted, compared with the FSi/30SiO_2–5TiO_2 coating. Therefore, the degradation rate can be improved by increasing TiO_2 addition ratio.

Combined with the wettability changes of FSi/30SiO_2–$x$$TiO_2$ coatings discussed above, it could be concluded that there is an evident correlation between photocatalysis and wettability variation. The changing trend of coating photocatalysis is consistent with its wettability variation, and they are both closely related to TiO_2 amount. As for coatings with similar superhydrophobicity, the superhydrophilicity would be obtained much faster and more easily with increasing TiO_2 amount after outdoor or UV exposure. Simultaneously, the photocatalytic performances would be enhanced with more TiO_2 addition amount.

The photocatalytic performances of coatings with different initial wettability characteristics are worth researching. The photocatalytic degradation performances of FSi/TiO_2 coatings with different SiO_2 addition ratios are shown in Fig. 8. The decolorization states of MB solution are also provided directly as inset pictures. It can be seen from Fig. 8 that coating samples with different initial wettability states have significantly different degradation performances even when the TiO_2 amount is the same. Interestingly, the degradation rates could also be enhanced with increasing SiO_2

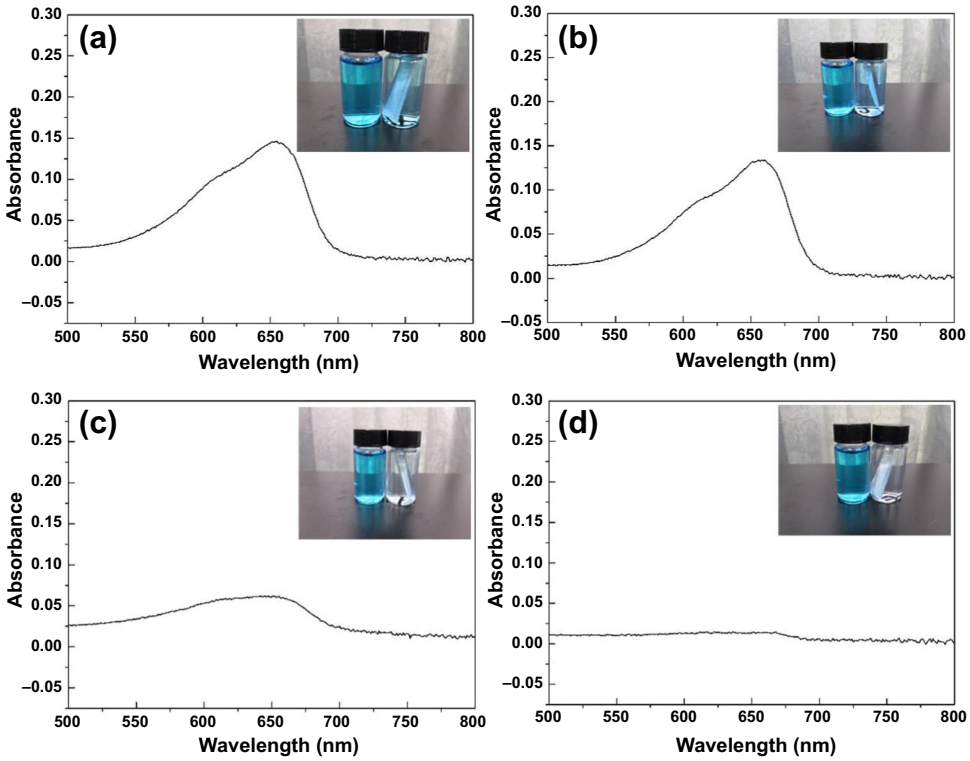

Fig. 7: The photocatalytic degradation performances of FSi/SiO_2 coatings with different TiO_2 addition ratios: (a) 1.5%; (b) 3%; (c) 5%; (d) 7.5%. (The corresponding inset figures show the decolorization of MB solution visually).

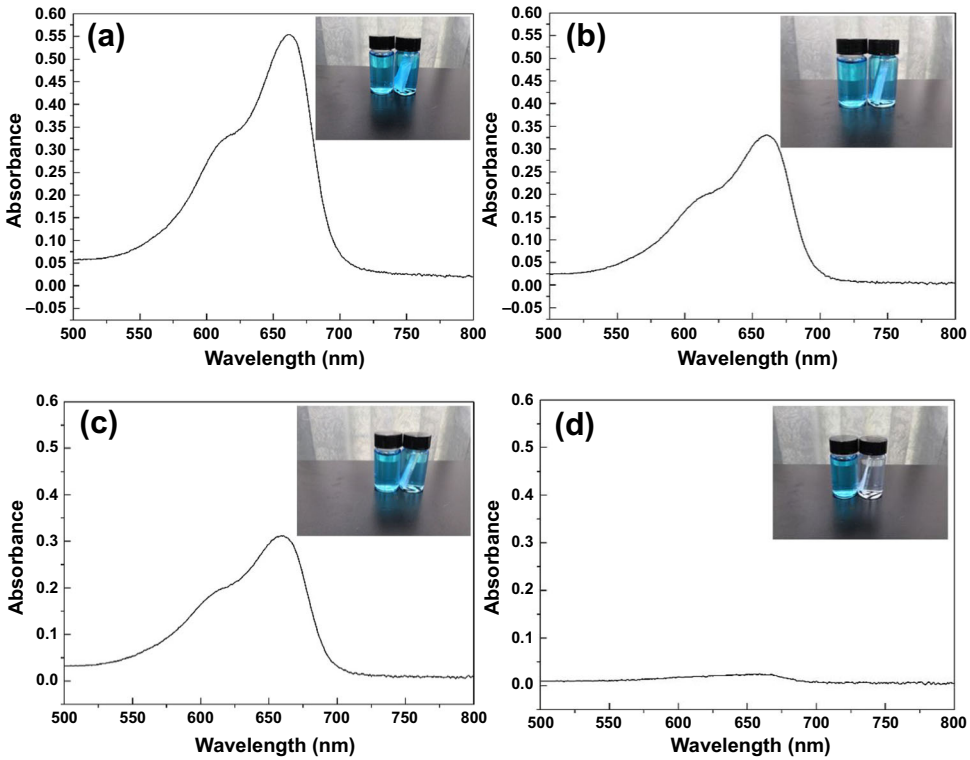

Fig. 8: The photocatalytic degradation performances of FSi/TiO_2 coatings with different SiO_2 addition ratios: (a) 20%; (b) 24%; (c) 28%; (d) 32%. (The corresponding inset figures show the decolorization of MB solution visually).

addition ratio. In addition, the degradation performance of the coating with 20% SiO_2 is very poor. The degradation rate is promoted when the SiO_2 addition ratio is increased to 24%. There is merely a small difference in the photocatalytic performances between FSi/5TiO_2–24SiO_2 and FSi/5TiO_2–28SiO_2 coatings. Apparently, the FSi/5TiO_2–28SiO_2 coating shows a relatively higher degradation rate. There is a great improvement of the degradation efficiency for the FSi/5TiO_2–32SiO_2 coating, compared with the above mentioned three samples.

The wettability changes of FSi/5TiO_2–$x$$SiO_2$ coatings discussed above should also be mentioned here again. Also, we know that their photocatalysis is not so consistent with the wettability variation. As mentioned above, the wettability of FSi/5TiO_2–24SiO_2 coating changes first. However, its photocatalytic performance is worse than that of FSi/5TiO_2–28SiO_2 and FSi/5TiO_2–32SiO_2. What is more, the superhydrophobicity of FSi/5TiO_2–32SiO_2 coating is so durable that it could withstand UV light and natural rain, which also elucidates its excellent photocatalytic performance. Although the coating samples with 20%, 24% and 28% of SiO_2 addition ratio could transform to superhydrophilic coatings much easier, the degradation rates are much worse than the stable superhydrophobic coating with 32% SiO_2. Based on Figs. 7a and 8a, we also know that the FSi/5TiO_2–24SiO_2 coating has a weaker photocatalytic ability than FSi/30SiO_2–1.5TiO_2, which means the degradation rate of the coating with more TiO_2 amount is not always much higher. Therefore, the coating photocatalytic performance is not only related to the TiO_2 addition amount, but also related to the coating initial hydrophobicity, which is determined by coating surface microstructure.

In addition, the photocatalytic activity of the FSi/5TiO_2–32SiO_2 coating was further tested by employing phenol, one type of typical organic pollutant. Figure 9 shows the degradation performance of FSi/5TiO_2–32SiO_2 coating on phenol. The phenol can be degraded by FSi/5TiO_2–32SiO_2 coating efficiently. Phenol concentration decreases to below 1 mg/L from 10 mg/L after 300 min of UV irradiation. However, the final removal efficiency reaches a limit of 92%, which means that the phenol is not able to be removed completely by our prepared coating.

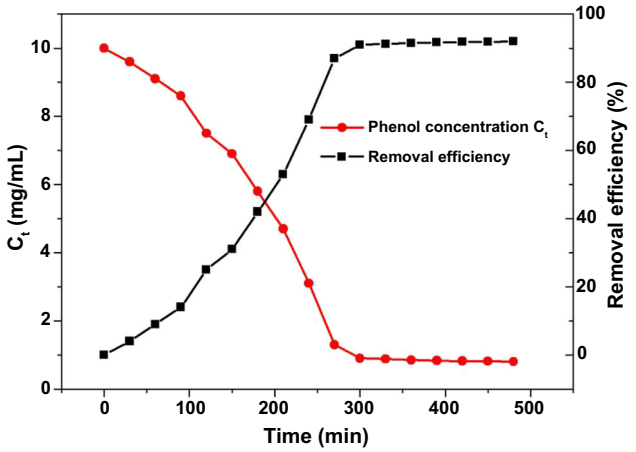

Fig. 9: The degradation performance of FSi/5TiO_2–32SiO_2 coating on phenol.

Morphology characteristic analysis and the self-cleaning performance

The well-known fact that the wettability and photocatalytic properties are closely related to coating surface morphology inspires us to explore the morphology characteristics of different coatings. Figure 10 shows the morphologies of FSi/SiO_2 coatings with different TiO_2 addition ratios. From the FESEM images, it can be seen that all the FSi/SiO_2–$x$$TiO_2$ coatings exhibit loose and porous structures. Micrometer-scale roughness formed due to the primary SiO_2 microparticle size and aggregated particle size. Roughness of a smaller scale was induced by submicron pore-like structure. It is known that the rough structures with different sizes are beneficial to the implementation of superhydrophobicity. Hence, initial superhydrophobic states could be shown in series of FSi/30SiO_2–$x$$TiO_2$ coatings. The morphologies of FSi/30SiO_2–$x$$TiO_2$ coatings (x = 1.5, 3, 5, 7.5) as shown in Figs. 7a, 7b, 7c and 7d, respectively, demonstrate that less TiO_2 addition could slightly promote the formation and homogeneity of rough structures with dual scale. When 5% of TiO_2 was doped into the coating system, continuous microscale convex structures can be separated by submicroscale porous structures. The cooperation and arrangement of microstructure and submicrostructure has an important influence on the water droplet form and the way it tends to move, which is the reason that the sliding angle of FSi/30SiO_2–5TiO_2 coating is lower than that of the others.

Similarly, the morphologies of FSi/TiO_2 coatings with different SiO_2 addition ratios are also examined and shown in Fig. 11. There are notable differences among the microstructures of the four coating samples with increasing SiO_2 addition amounts. When the SiO_2 addition ratio is 20%, there appears a characteristic of a relatively flat surface. A few micron protuberances surrounded by smooth resin film distribute unevenly on the entire coating surface and larger aggregates of SiO_2 particles with loose construction can be found. It is obvious that the surface structure of FSi/5TiO_2–20SiO_2 coating sample is not favorable to achieve superhydrophobicity. There are great changes in the surface morphology when the SiO_2 addition ratio is increased to 24% from 20%. A uniform loose and porous microstructure is obtained on the FSi/5TiO_2–24SiO_2 coating sample. Ordered convex and concave microstructures are displayed in an alternating distribution. For all that, the sizes of surface protuberance and hollow structures are in a similar submicroscale. Although the surface structure with a single-scale

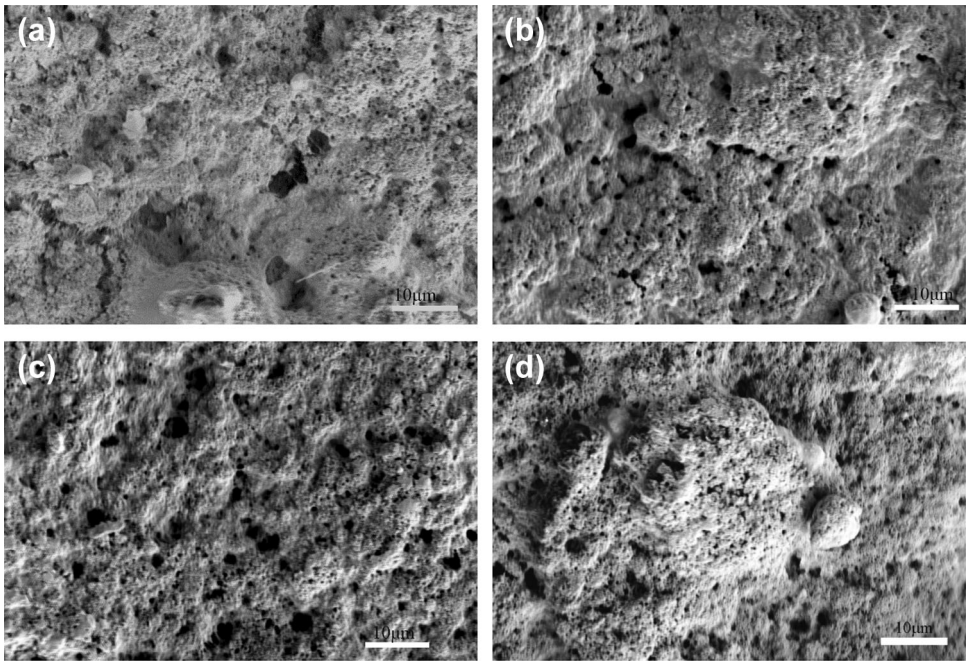

Fig. 10: The morphologies of FSi/SiO_2 coatings with different TiO_2 addition ratios: (a) 1.5%; (b) 3%; (c) 5%; (d) 7.5%.

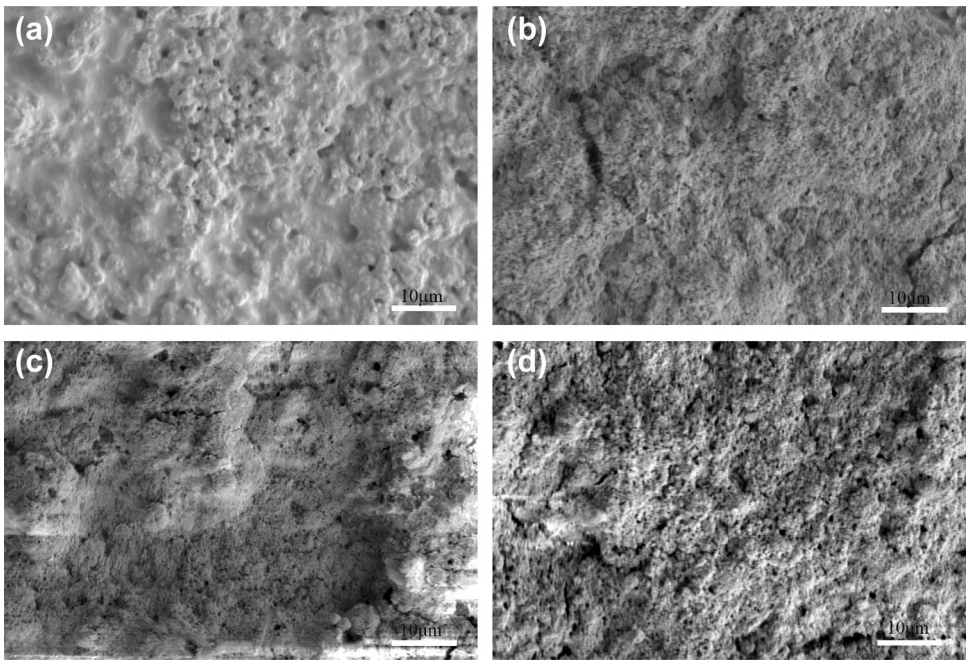

Fig. 11: The morphologies of FSi/TiO_2 coatings with different SiO_2 addition ratios: (a) 20%; (b) 24%; (c) 28%; (d) 32%.

roughness possesses a water contact angle of larger than 150°, the water droplets could not easily roll off the surface, which is in good agreement with the experimental results. In Fig. 11c, the microaggregates appear with continued increase of the SiO_2 addition ratio, and superhydrophobicity is obtained on the FSi/$5TiO_2$–$28SiO_2$ coating sample with a sliding angle less than 10°. In addition, there is another significant change when SiO_2 addition ratio is increased to 32% from 28%. The loose and porous microstructure of FSi/$5TiO_2$–$32SiO_2$ presents a more homogeneous state, showing a better superhydrophobicity as a result. Based on the analysis above, it can be concluded that the SiO_2 addition plays an important role in constructing a superhydrophobic structure.

It is doubtless that the wettability change and photocatalysis evolution are closely related to the initial wetting states of the coating, which is mainly affected by the coating surface microstructure. In order to represent the wetting states more directly, possible wetting states of the prepared coatings are provided as schematic diagrams shown in Fig. 12. The spreading state of water droplets on the coating surfaces is displayed more intuitively, and four representative states are given. A partial wetting state is shown in Fig. 12a, the water contact angle of which is the closest to the ideal equilibrium static contact angle raised by Young's equation. This is because the relatively smooth coating surface is composed of homogeneous resin since most of doped particles are buried inside of the resin matrix. There would be some certain rough structures on the coating when the filler loading level is increased, which could change the wettability of the coating surface. Figure 12b shows the classic Wenzel model of wetting state on a microscopic rough surface, which exhibits a high apparent contact angle and a high sliding angle. The water would fill the rough asperities of the coating surface, and the solid–liquid adhesion is increased due to the pinning effects. However, the classic Cassie–Baxter model is more suitable to explain the wettability for those porous surfaces with high roughness. The classic Cassie–Baxter state is illustrated in Fig. 12d. Air pockets formed on the contact plane of the liquid and solid phase can lead to a small fraction of liquid–solid contact area, which helps to decrease the water adhesion on the coating surface; thus, the water droplet can roll off easily. Besides, there also exists a semi Cassie–Baxter wetting state, shown in Fig. 12c, indicating that an intermediate hybrid state appears as a Cassie–Baxter state in microscale and a Wenzel state in submicroscale. Water droplets would penetrate partially in the rough structure.

Based on the discussions above, it can be concluded that the microstructures of FSi/30SiO_2–$x$$TiO_2$ coatings are more conformed to a semi Cassie–Baxter wetting model. During the UV illumination or outdoor exposure process, it is believed that the photoinduced hydrophilicity and photocatalysis are carried out simultaneously. The electron–hole pairs created on the coating surface could react with Ti^{4+} and O^{2-}, respectively. The dissociative adsorption of water on the reaction products of oxygen vacancy would promote the formation of chemical adsorbed water layers. Meanwhile, the electron–hole pairs created on the coating surface would react with O_2 and OH^-, respectively, and the highly active superoxide ion and hydroxyl radical are thus generated, which can degrade the pollutants into small molecule compounds such as CO_2 and H_2O. Both of the above reaction paths can lead to water molecular penetration into the loose and porous coating surface. Therefore, a wettability model changed into the Wenzel state could take place in the initial stage of UV illumination or outdoor exposure. Hydrophilic and even superhydrophilic properties are gradually shown on the coating with increasing irradiation or exposure time. Evidently, the photoinduced hydrophilicity and photocatalysis of FSi/30SiO_2–$x$$TiO_2$ coating series are enhanced by the higher TiO_2 content.

However, the FSi/5TiO_2–$x$$SiO_2$ coatings would show completely different wetting states depending on the addition ratio of SiO_2. According to the examples of wetting states listed in Fig. 12, it is found that the FSi/5TiO_2–$x$$SiO_2$ (x = 20, 24, 28, 32) correspond to wetting models of Figs. 12a, 12b, 12c and 12d, respectively. From the perspectives of wettability change, the superhydrophobicity of coating surface with an initial Wenzel wetting state is more likely to weaken first, which is shown on the coating surface of FSi/5TiO_2–24SiO_2. Next comes the surface of FSi/5TiO_2–28SiO_2 coating with an initial semi Cassie–Baxter wetting state; it would change into a Wenzel state rapidly under UV irradiation or outdoor exposure. Once a Wenzel wetting state is formed, the coating surface

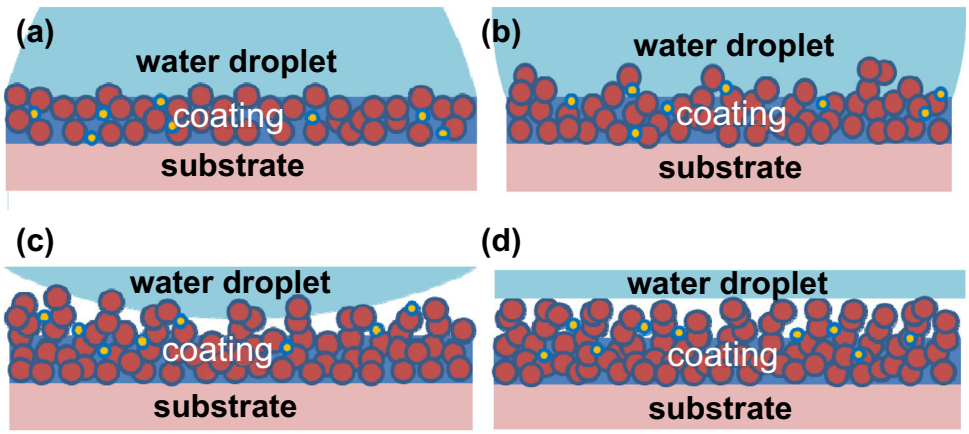

Fig. 12: Possible wetting states of the prepared coatings: (a) partial wetting state; (b) classic Wenzel state; (c) semi Cassie–Baxter state; (d) classic Cassie–Baxter state. (Here the red balls are referred to as SiO_2 particles and the yellow balls are TiO_2 nanoparticles) (Color figure online).

Table 1: The surface roughness, microstructure, hydrophilic transition under UV, and photocatalytic performance of prepared coatings.

Composition	Roughness (μm)	Wetting model	Wettability transition (CA value) under UV	MB concentrations (mg/L) (214 h)
FSi/30SiO_2–1.5TiO_2	6.297	Semi Cassie–Baxter state	129.26° at the 214th hour	0.973
FSi/30SiO_2–3TiO_2	7.202	Semi Cassie–Baxter state	0° at the 190th hour	1.013
FSi/30SiO_2–5TiO_2	8.248	Semi Cassie–Baxter state	48° at the 176th hour	0.549
FSi/30SiO_2–7.5TiO_2	9.934	Semi Cassie–Baxter state	0° at the176th hour	0.297
FSi/5TiO_2–20SiO_2	4.451	Partial wetting state	56.41° at the 190th hour	3.426
FSi/5TiO_2–24SiO_2	5.511	Classic Wenzel state	0° at the 80th hour	2.121
FSi/5TiO_2–28SiO_2	7.04	Semi Cassie–Baxter state	36.65° at the 152th hour	2.004
FSi/5TiO_2–32SiO_2	10.011	Classic Cassie–Baxter state	154.74° at the 214th hour	0.353

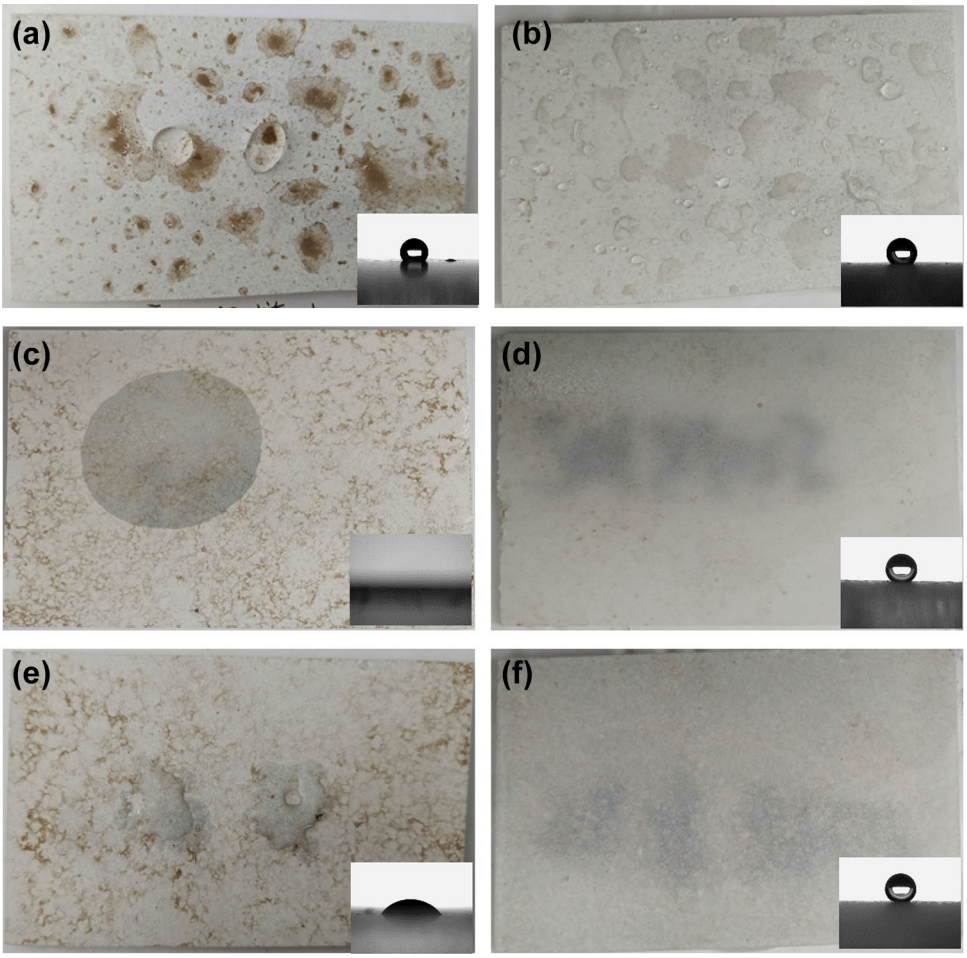

Fig. 13: The pollution conditions and self-cleaning performances of three typical coatings with different surface characteristics: (a, b) superhydrophobic FSi/SiO_2 coating; (c, d) photoinduced superhydrophilic FSi/5TiO_2–28SiO_2 coating; (e, f) superhydrophobic photocatalytic FSi/5TiO_2–32SiO_2 coating.

would become hydrophilic and further superhydrophilic in a short time, which is due to the photoinduced hydrophilicity and photocatalysis effect brought by TiO_2 particles. The water molecule produced from the decomposition reactions by TiO_2 particles during the UV irradiation would form a continuous unit of water layers with the water on the coating surface. Therefore, the water droplets could easily pass through the water film channel and spread out on the coating surface. However, it seems more difficult for FSi/5TiO_2–20SiO_2 coating surface to transform into a hydrophilic coating although it initially exhibits a partial

Table 2: The pollution performance and hydrophobicity recovery of three typical coatings with different surface characteristics.

Coating composition	FSi/SiO_2	$FSi/5TiO_2–28SiO_2$	$FSi/5TiO_2–32SiO_2$
Initial hydrophobicity (CA/SA)	156.25°/5.5°	154.92°/6°	158.37°/3°
Pollution performance	Obvious discontinuous stains	Continuous dusts	Continuous dusts
Hydrophobicity loss after outdoor exposure (CA)	130.1°	0°	59°
Hydrophobicity recovery after heating (CA/SA)	143°	152.79°/9.5°	157.01°/6°

wetting state. The characteristics of photoinduced hydrophilicity and photocatalysis from TiO_2 particles are weakened since they are embedded inside the compact resin film. More importantly, the water could not easily penetrate into the coating owing to its smooth and dense surface microstructure composed mostly of resin. Actually, it is proven that an excellent initial superhydrophobicity is necessary to prevent hydrophobicity decay during UV irradiation. A classic Cassie–Baxter wetting state forms on the surface of $FSi/5TiO_2–32SiO_2$ coating. It should take more time for the Cassie–Baxter wetting state to transform to Wenzel state due to complex rough surface structure. The microscopic hydrophilic zone would not influence the coating's macroscopic hydrophobicity. As mentioned above, the photocatalytic degradation performance is improved by increasing the surface hydrophobicity, which might be attributed to increased reactive and exposed areas brought by the structures with multilevel roughness. Surface roughness values were tested by an optical profilometer. The surface roughness values of those prepared coating samples are listed in Table 1. The photocatalysis effect and coating surface roughness are both influenced by increasing the TiO_2 addition amount. For those $FSi/30SiO_2–xTiO_2$ coating samples, the coating surface roughness values show a rising tendency with TiO_2 addition increasing from 1.5 to 7.5%. It could also be seen that the coating surface roughness values increase greatly with SiO_2 addition. The roughness value of $FSi/5TiO_2–32SiO_2$ coating increases up to over two times that of $FSi/5TiO_2–20SiO_2$ coating. Therefore, the roughness value proves to play a decisive role in the formation process of a superhydrophobic microstructure. In addition, the wetting model, wettability transition under UV irradiation, as well as MB concentrations decomposed for FSi/SiO_2 and FSi/TiO_2 coating series are summarized in Table 1. Therefore, the hydrophobicity and photocatalytic performances of different coatings can be compared intuitively.

The self-cleaning performances of superhydrophobic photocatalytic $FSi/5TiO_2–32SiO_2$ coating were investigated and compared with the superhydrophobic FSi/SiO_2 coating and photoinduced superhydrophilic $FSi/5TiO_2–28SiO_2$ coating. All three coatings were subjected to outdoor exposure for 3 months of a pollution accumulated period in winter. Figure 13 shows the pollution conditions and self-cleaning performances of the three typical coatings with different surface characteristics including superhydrophobic surface, photoinduced superhydrophilic surface and the superhydrophobic photocatalytic surface.

The superhydrophobic FSi/SiO_2 coating is contaminated by obvious discontinuous stains due to the impact of raindrops containing organic pollutants. The original superhydrophobicity of the FSi/SiO_2 coating has been lost, whose contact angle is about 130.1°. The pollution condition of the photoinduced superhydrophilic $FSi/5TiO_2–28SiO_2$ coating is quite different from that of the superhydrophobic coating. Pollutants on the photoinduced superhydrophilic surface are shown as dusts. The water dropped can be infiltrated into the surface showing a completely hydrophilic state with a contact angle of 0°. The $FSi/5TiO_2–32SiO_2$ coating with initial superhydrophobic and photocatalytic properties shows a more similar pollution condition to the photoinduced superhydrophilic coating, while the WCA value is tested as 59° on the $FSi/5TiO_2–32SiO_2$ coating after exposure. Therefore, it could be learned that the superhydrophobic coating with photocatalysis would lose its superhydrophobicity sooner or later, which is determined by the initial superhydrophobicity and its durability. In addition, the self-cleaning performance and hydrophobicity recovery of the three typical surfaces were also explored. After being cleaned by running water, the contaminated area of the superhydrophobic FSi/SiO_2 coating surface changes from hydrophobic to hydrophilic, although most of the visible pollutants can be removed. The WCA could only be recovered as 143° after drying the coating at 80°C in an oven. It is suggested that some organic pollutants could adhere to the superhydrophobic surface deeply and cannot be easily cleaned. For the other two $FSi/TiO_2–SiO_2$ coatings studied, it is found that superhydrophilicity is obtained after cleaning the dust floated on the surfaces. However, the superhydrophobicity can be returned to the original level after drying the coating at 80°C. It is indicated that the prepared $FSi/5TiO_2–SiO_2$ coating series with durable superhydrophobicity exhibits excellent self-cleaning and superhydrophobicity recovery performances. The specific performances of pollution states and hydrophobicity recovery for three typical coatings with different surface characteristics are shown in Table 2. The initial hydrophobicity, pollution performance, hydrophobicity loss and recovery can be compared more easily.

Conclusions

In summary, photocatalytic TiO_2 particles were introduced into an FSi/SiO_2 coating system in order to prepare a superhydrophobic coating with photocatalytic properties. Effects of TiO_2 amount and the initial hydrophobicity on the coating wettability change with the UV irradiation and outdoor exposure time were investigated, respectively. Evolution patterns of wettability and photocatalytic activity were shown in our study. It has been found that more TiO_2 addition could promote the coating transformation from superhydrophobic to superhydrophilic. However, all the FSi/30SiO_2 coating series could change into superhydrophilic even with only 1.5% TiO_2. Besides, the hydrophobicity and photocatalytic activity can be improved by increasing SiO_2 addition ratio. The coatings with less SiO_2 present poor photocatalytic activity. The FSi/5TiO_2–32SiO_2 coating with a more durable initial superhydrophobicity can maintain its initial wettability, while its photocatalytic property is better than that of the contrast coating series. It is believed that the coating with a Cassie–Baxter surface structure shows a better photocatalysis through analyzing the surface microstructure. The prepared superhydrophobic and photocatalytic coating in this work exhibits a good practical self-cleaning performance because of the good photodegradation effect on the organic pollutants in the environment. Moreover, the superhydrophobicity of the FSi/5TiO_2–SiO_2 coating is able to be recovered, compared with the superhydrophobic FSi/SiO_2 coatings.

Acknowledgments The authors thank State Grid Corporation of China (520626170025) for its financial support.

References

1. Milionis, A, Loth, E, Bayer, IS, ''Recent Advances in the Mechanical Durability of Superhydrophobic Materials.'' *Adv. Colloid Interface Sci.*, **229** 57–79 (2016)
2. Yu, N, Xiao, X, Ye, Z, Pan, G, ''Facile Preparation of Durable Superhydrophobic Coating with Self-cleaning Property.'' *Surf. Coat. Technol.*, **347** 199–208 (2018)
3. Ragesh, P, Ganesh, VA, Naira, SV, Nair, AS, ''A Review on 'Self-cleaning and Multifunctional Materials.''' *J. Mater. Chem. A*, **2** 14773–14797 (2014)
4. Wang, R, Hashimoto, K, Fujishima, A, Chikuni, M, Kojima, E, Kitamura, A, et al., ''Light-Induced Amphiphilic Surfaces.'' *Nature*, **388** (6641) 431–432 (1997)
5. Liu, K, Tian, Y, Jiang, L, ''Bio-inspired Superoleophobic and Smart Materials: Design, Fabrication, and Application.'' *Prog. Mater. Sci.*, **58** (4) 503–564 (2013)
6. Makaryan, IA, Sedov, IV, Mozhaev, PS, ''Current State and Prospects of Development of Technologies for the Production of Superhydrophobic Materials and Coatings.'' *Nanotechnol. Russ.*, **11** (11–12) 679–695 (2016)
7. Nguyen-Tri, P, Tran, HN, Plamondonc, CO, et al., ''Recent Progress in the Preparation, Properties and Applications of Superhydrophobic Nano-based Coatings and Surfaces: A Review.'' *Prog. Org. Coat.*, **132** 235–256 (2019)
8. Lu, Y, et al., ''Robust Self-cleaning Surfaces that Function When Exposed to Either Air or Oil.'' *Science*, **347** (6226) 1132–1135 (2015)
9. Xie, WY, et al., ''A Superhydrophobic and Self-cleaning Photoluminescent Protein Film with High Weatherability.'' *Chem. Eng. J.*, **326** 436–442 (2017)
10. Bakea, A, Merah, N, Matin, A, Gondal, M, Qahtan, T, Abu-Dheir, N, ''Preparation of Transparent and Robust Superhydrophobic Surfaces for Self-cleaning Applications.'' *Prog. Org. Coat.*, **122** 170–179 (2018)
11. Latthe, SS, Sutar, RS, Kodag, VS, et al., ''Self-cleaning Superhydrophobic Coatings: Potential Industrial Applications.'' *Prog. Org. Coat.*, **128** 52–58 (2019)
12. Bayer, I, ''On the Durability and Wear Resistance of Transparent Superhydrophobic Coatings.'' *Coatings*, **7** (1) 12–35 (2017)
13. Latthe, SS, Terashima, C, Nakata, K, et al., ''Superhydrophobic Surfaces Developed by Mimicking Hierarchical Surface Morphology of Lotus Leaf.'' *Molecules*, **19** (4) 4256–4283 (2014)
14. Zhang, M, Feng, S, Wang, L, Zheng, Y, ''Lotus Effect in Wetting and Self-cleaning.'' *Biotribology*, **5** 31–43 (2016)
15. Varshney, P, Lomga, J, Gupta, PK, Mohapatra, SS, Kumar, A, ''Durable and Regenerable Superhydrophobic Coatings for Aluminium Surfaces with Excellent Self-cleaning and Anti-fogging Properties.'' *Tribol. Int.*, **119** 38–44 (2018)
16. Zhang, X, Guo, Y, Zhang, Z, Zhang, P, ''Self-cleaning Superhydrophobic Surface Based on Titanium Dioxide Nanowires Combined with Polydimethylsiloxane.'' *Appl. Surf. Sci.*, **284** 319–323 (2013)
17. Pawar, PG, Xing, R, Kambale, RC, Kumar, AM, et al., ''Polystyrene Assisted Superhydrophobic Silica Coatings with Surface Protection and Self-cleaning Approach.'' *Prog. Org. Coat.*, **105** 235–244 (2017)
18. Zeng, W, Chen, J, Yang, H, Deng, L, ''Robust Coating with Superhydrophobic and Self-cleaning Properties in Either Air or Oil Based on Natural Zeolite.'' *Surf. Coat. Technol.*, **309** 1045–1051 (2017)
19. Cully, P, Karasu, F, Müller, L, Jauzein, T, Leterrier, Y, ''Self-cleaning and Wear-Resistant Polymer Nanocomposite Surfaces.'' *Surf. Coat. Technol.*, **348** 111–120 (2018)
20. Zheng, S, Li, C, Fu, Q, Hua, W, Xiang, T, et al., ''Development of Stable Superhydrophobic Coatings on Aluminum Surface for Corrosion-Resistant, Self-cleaning, and Anticing Applications.'' *Mater. Des.*, **93** 261–270 (2016)
21. Li, X, Li, H, Huang, K, Zou, H, et al., ''Durable Superamphiphobic Nano-silica/Epoxy Composite Coating via Coaxial Electrospraying Method.'' *Appl. Surf. Sci.*, **436** 283–292 (2018)
22. Chen, L, Guo, Z, Liu, W, ''Biomimetic Multi-functional Superamphiphobic FOTS–TiO_2 Particles Beyond Lotus Leaf.'' *ACS Appl. Mater. Interfaces*, **8** 27188–27198 (2016)
23. Nakata, K, Fujishima, A, ''TiO_2 Photocatalysis: Design and Applications.'' *J. Photochem. Photobiol. C Photochem. Rev.*, **13** 169–189 (2012)
24. Ding, X, Zhou, S, Wu, L, Gu, G, et al., ''Formation of Supra-amphiphilic Self-cleaning Surface Through Sun-Illumination of Titania-Based Nanocomposite Coatings.'' *Surf. Coat. Technol.*, **205** 2554–2561 (2010)
25. Xie, W, Xiao, X, Zhao, Y, Zhang, W, ''Preparation of Hydrophobic SiO_2@(TiO_2/MoS_2) Composite Film and Its

Self-cleaning Properties.'' *J. Coat. Technol. Res.*, **14** (1) 1–12 (2017)
26. Kim, SM, In, I, Park, SY, ''Study of Photo-induced Hydrophilicity and Self-cleaning Property of Glass Surfaces Immobilized with TiO_2 Nanoparticles Using Catechol Chemistry.'' *Surf. Coat. Technol.*, **294** 75–82 (2016)
27. Chekini, M, Mohammadizadeh, MR, Allaei, SMV, ''Photocatalytic and Superhydrophilicity Properties of N-Doped TiO_2 Nanothin Films.'' *Appl. Surf. Sci.*, **257** 7179–7183 (2011)
28. Byrne, C, Subramanian, G, Pillai, SC, ''Recent Advances in Photocatalysis for Environmental Applications.'' *J. Environ. Chem. Eng.*, **6** 3531–3555 (2018)
29. Stepien, M, Saarinen, JJ, Teisal, H, Tuominen, M, et al., ''Surface Chemical Analysis of Photocatalytic Wettability Conversion of TiO_2 Nanoparticle Coating.'' *Surf. Coat. Technol.*, **208** 73–79 (2012)
30. Li, W, Guo, T, Meng, T, Huang, Y, et al., ''Enhanced Reversible Wettability Conversion of Micro-nano Hierarchical TiO_2/SiO_2 Composite Films Under UV Irradiation.'' *Appl. Surf. Sci.*, **283** 12–18 (2013)
31. Miyauchi, M, Kied, N, Hishit, S, Mitsuhashi, T, ''Reversible Wettability Control of TiO_2 Surface by Light Irradiation.'' *Surf. Sci.*, **511** 401–407 (2002)
32. Ding, Y, Xu, B, Ge, F, Cai, Z, ''Robust Superhydrophobic, and Photocatalytic Cotton Fabrics Based on TiO_2–SiO_2–PDMS Composite Coating.'' *Key Eng. Mater.*, **671** 225–230 (2016)
33. Xu, QF, Liu, Y, Lin, F-J, Mondal, B, Lyons, AM, ''Superhydrophobic TiO_2−Polymer Nanocomposite Surface with UV Induced Reversible Wettability and Self-cleaning Properties.'' *ACS Appl. Mater. Interfaces*, **5** 8915–8924 (2013)
34. Crick, CR, Bear, JC, Kafizas, A, Parkin, IP, ''Superhydrophobic Photocatalytic Surfaces Through Direct Incorporation of Titania Nanoparticles into a Polymer Matrix by Aerosol Assisted Chemical Vapor Deposition.'' *Adv. Mater.*, **24** 3505–3508 (2012)
35. Kamegawa, T, Shimizu, Y, Yamashita, H, ''Superhydrophobic Surfaces with Photocatalytic Self-cleaning Properties by Nanocomposite Coating of TiO_2 and Polytetrafluoroethylene.'' *Adv. Mater.*, **24** 3697–3700 (2012)
36. Park, EJ, Yoon, HS, Kim, DH, Kim, YH, Kim, YD, ''Preparation of Self-cleaning Surfaces with a Dual Functionality of Superhydrophobicity and Photocatalytic Activity.'' *Appl. Surf. Sci.*, **319** 367–371 (2014)
37. Ratova, M, Kelly, PJ, West, GT, ''Superhydrophobic Photocatalytic PTFE – Titania Coatings Deposited by Reactive pDC Magnetron Sputtering from a Blended Powder Target.'' *Mater. Chem. Phys.*, **190** 108–113 (2017)
38. Zhao, Y, Liu, Y, Xu, QF, Barahman, M, Lyons, AM, Catalytic, A, ''Self-cleaning Surface with Stable Superhydrophobic Properties: Printed PDMS Arrays Embedded with TiO_2 Nanoparticles.'' *ACS Appl. Mater. Interfaces*, **7** (4) 2632 (2014)
39. Ding, X, Zhou, S, Gua, G, Wu, L, ''A Facile and Large-Area Fabrication Method of Superhydrophobic Self-cleaning Fluorinated Polysiloxane/TiO_2 Nanocomposite Coatings with Long-Term Durability.'' *J. Mater. Chem.*, **21** 6161–6164 (2011)
40. Wu, Y, Li, X, Mi, C, Zong, L, Wang, X, ''Preparation and Characterization of Perfluorine–SiO_2 Nanoparticles and Superhydrophobic Fluorosilicone/Silica Hybrid Composite Coating.'' *Appl. Phys. A*, **125** 250 (2019)
41. Qing, Y, Yang, C, Yu, N, Shang, Y, et al., ''Superhydrophobic TiO_2/Polyvinylidene Fluoride Composite Surface with Reversible Wettability Switching and Corrosion Resistance.'' *Chem. Eng. J.*, **290** 37–44 (2016)
42. Xu, B, Ding, J, Feng, L, Ding, Y, Ge, F, Cai, Z, ''Self-cleaning Cotton Fabrics via Combination of Photocatalytic TiO_2 and Superhydrophobic SiO_2.'' *Surf. Coat. Technol.*, **262** 70–76 (2015)
43. Alfieri, I, Lorenzi, A, Ranzenigo, L, Lazzarini, L, et al., ''Synthesis and Characterization of Photocatalytic Hydrophobic Hybrid TiO_2–SiO_2 Coatings for Building Applications.'' *Build. Environ.*, **111** 72–79 (2017)